Available online at www.sciencedirect.com
SCIENCE DIRECT®
Mechanics of Materials 38 (2006) 463–474
MECHANICS OF MATERIALS
www.elsevier.com/locate/mechmat

Superelastic and cyclic response of NiTi SMA at various strain rates and temperatures

Sia Nemat-Nasser [a,*], Wei-Guo Guo [b]

[a] Center of Excellence for Advanced Materials, Department of Mechanical and Aerospace Engineering, University of California, San Diego, La Jolla, CA 92093-0416, USA
[b] Department of Aircraft Engineering (118#), Northwestern Polytechnical University, Xi'an City, Shaanxi Province, 710072, PR China

Received 28 October 2004; received in revised form 19 July 2005

Abstract

To characterize the thermomechanical response, especially the superelastic behavior of NiTi shape-memory alloys (SMAs) at various temperatures and strain rates, we have performed a series of both quasi-static and dynamic uniaxial compression tests on cylindrical samples, using an Instron servohydraulic testing machine and UCSD's enhanced Hopkinson technique. Strain rates from 10^{-3}/s to about 4200/s are achieved, at initial temperatures in the range of 77–400 K. The influence of the annealing temperature on the fatigue response is also examined. A few noteworthy conclusions are as follows: (1) the transformation stress and the dissipated energy of NiTi SMAs depend on the annealing temperature; (2) in cyclic loading, the dissipated energy over a cycle tends to a minimum stable value, and cyclic loading leads to a stable superelastic behavior of the alloy; (3) repeated dynamic tests of the alloy produce smaller changes in the shape of the superelastic loop and in the dissipated energy than do the quasi-static cyclic tests; and (4) the superelastic behavior of this material has stronger sensitivity to temperature than to strain rate; at very high loading rates, NiTi SMAs show properties similar to ordinary steels, as has been established by the first author and coworkers.

Keywords: NiTi shape-memory alloys; Superelasticity; Dissipated energy; Strain rate; Fatigue; Temperature

1. Introduction

Depending on the temperature, in general, SMAs can exist in two different crystal structures, the martensitic phase (at low temperatures) and the austenitic phase (at high temperatures). The parent austenitic phase has a cubic lattice (B2) while the martensitic phase is monoclinic (B19′) (Otsuka and Ren, 1999), consisting of only lattice twins (see Fig. 1). When a NiTi SMA in the martensitic phase is heated, it begins to change into the austenitic phase. This phenomenon starts at a temperature denoted by A_s, and is complete at a temperature denoted by A_f. When an austenitic NiTi SMA is cooled, it begins to return to its martensitic structure at a temperature denoted by M_s, and the process is complete at a temperature denoted by M_f. The difference between the transformation

* Corresponding author. Tel.: +1 858 534 4914; fax: +1 858 534 2727.
E-mail address: sia@ucsd.edu (S. Nemat-Nasser).

0167-6636/$ - see front matter © 2005 Elsevier Ltd. All rights reserved.
doi:10.1016/j.mechmat.2005.07.004

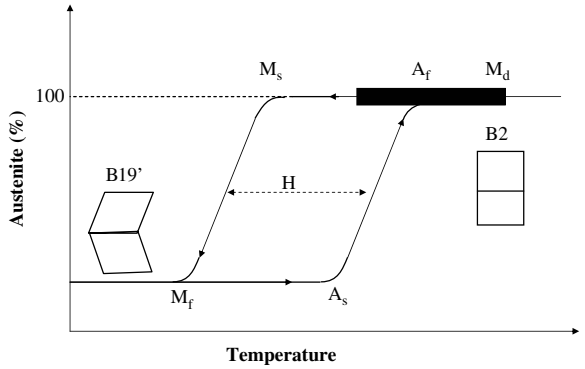

Fig. 1. Phase transformation in NiTi SMAs.

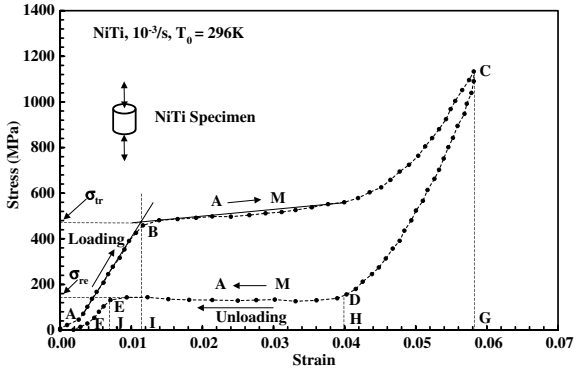

Fig. 2. Superelastic effect of NiTi SMA after 42% cold work followed by 30 min annealing 823 K.

temperatures in heating and cooling is called the hysteresis temperature. In practice, the hysteresis temperature is generally defined as the difference between the temperatures at which the material is 50% transformed to the austenite upon heating and 50% transformed back to the martensite upon cooling; this is denoted by H in Fig. 1.

The chemical composition and the metallurgical treatment have a significant effect on the transformation temperatures. When a NiTi SMA is stressed at a temperature close to A_f, it can display superelastic (or pseudoelasticity) behavior which is often defined in terms of the ability of the material to return to its original shape upon unloading, after a substantial deformation. This stems from the stress-induced martensite formation, since stress can produce the martensitic phase at a temperature higher than M_s, where macroscopic deformation is accommodated by the formation of martensites. When the applied stress is released, the martensitic phase transforms back into the austenitic phase and the specimen returns back to its original shape. Fig. 2 represents a typical experimental result. In this figure, a superelastic NiTi SMA is strained up to 6%, which is several times greater than the elastic limit of ordinary metal alloys, and then unloaded, showing no permanent deformations. This is, however, only observed over a specific temperature and strain range. The heavy black bar in Fig. 1 suggests the temperature range on which superelastic behavior can occur. The highest temperature at which martensitic transformation can no longer be induced by an applied stress, is denoted by M_d. Above the M_d temperature, NiTi SMAs behave as ordinary metals. Below the A_s temperature, they deform while in the martensitic phase, and usually do not recover their original shape upon unloading. However, if they are then heated to a certain temperature, the NiTi SMAs can recover and attain their original shape. The stress-induced superelastic behavior appears in a temperature range from near A_f up to M_d, as is suggested in Fig. 1. When a NiTi SMA is tested at a temperature below A_f or above M_d, the measured surface temperature distribution of the specimen is uniform, indicating the homogeneity of the process of phase transformation. Deformation at a temperature T, with $A_f < T < M_d$, leads to a heterogeneous surface temperature, pointing out that the development of martensitic transformation is non-homogeneous (Gadaj et al., 2002) in this temperature range.

2. Superelastic behavior of NiTi SMA

A sample of NiTi that has been annealed at 823 K for 30 min is deformed in uniaxial compression at a strain rate of 10^{-3}/s and an initial temperature 296 K. The resulting engineering stress–engineering strain curve is displayed in Fig. 2. The sample at room temperature, 296 K, is in an austenitic phase. The initial AB segment of the stress–strain curve in Fig. 2 is the elastic deformation of the austenitic phase (parent phase). Close to point B, microscopic martensites are generated preferentially within the parent phase, because of stressing. In the initial BC segment, some plastic deformations may accompany the martensitic phase transformation. This plastic deformation is produced in order to accommodate locally the resulting martensitic phase (Hosogi et al., 2002). Upon further deformation, extensive stress-induced transformation takes place in the BC segment, at essentially a constant stress. At point C, the maximum stress-induced

phase-transformation strain is attained. The CD segment corresponds to the elastic unloading of the martensitic phase. The reverse transformation starts around point D and is complete around point E. The reverse transformation on the DE segment occurs at almost a constant stress. The EF segment is the elastic unloading of the austenites. At F, a small permanent residual strain remains, representing the plastic deformation in the martensitic phase. This residual plastic strain has actually occurred in the BC segment. Its magnitude mainly depends on the maximum total strain and the deformation temperature. Basically, the deformation at a temperature close to or slightly greater than A_f could lead to a small residual strain. Also, the treatment conditions and the chemical composition of the material affect this irrecoverable strain. The annealing temperature is found to have a great effect on the superelastic behavior of NiTi SMAs. In particular, the maximum plateau strain (the forward stress-induced transformation) increases with increasing annealing temperature, being 9% for specimens annealed at 873 K (Huang and Liu, 2001). Miller and Lagoudas (2001) point out that the level of cold work and the annealing temperature affect the transformation characteristics of the thermally induced phase transformation under a constant applied stress, specifically the transformation strain and transformation-induced plastic strain.

In the past decade, the thermomechanical response and superelastic behavior of NiTi SMAs under different conditions have been extensively studied (Shaw and Kyriakides, 1995; Gall et al., 1999; Otsuka and Wayman, 1998). The dynamic response of NiTi SMAs has also been studied to a certain extent. Tobushi et al. (1998) carried out dynamic tensile tests, and found that, for $\dot{\varepsilon} \geqslant 10\%/\min$, the stress and temperature for the martensitic transformation increase with an increase in $\dot{\varepsilon}$ in the loading process, but the reverse transformation stress and temperature decrease in the unloading process. The compressive stress–strain behavior of SMAs depends on the strain rate, and under dynamic loading conditions, it displays an open hysteresis loop because of the resulting residual strain which however, may disappear at room temperature, and, after a few seconds to several hours, the recovery may be complete (Chen et al., 2001). More recently, Nemat-Nasser et al. (2005a,b) have experimentally established the strain-rate sensitivity of the transition stress for stress-induced martensite formation, and the existence of a critical strain rate which determines the deformation mechanism of austenitic SMAs. This is in contrast to Liu et al. (1999a,b) who point out that, when the strain rate changes from 3×10^{-4} to 3000/s, the characteristics of the stress–strain curve for martensitic NiTi are insensitive to the strain rate, suggesting that the deformation mechanism does not change with the strain rate. Recently, a one-dimensional polycrystalline SMA bar was studied numerically and experimentally using a Hopkinson bar by Lagoudas et al. (2003). The energy dissipation calculation for both detwinning of the martensite and stress-induced phase transformation showed that the energy can be reduced by 80–90%, suggesting that SMAs can be used effectively in shock-absorbing devices.

Over the past few years, an experimental program to study the dynamic response of NiTi SMAs has been initiated by Nemat-Nasser and coworkers in an effort to understand the dynamic behavior of these alloys. The present work has been an integral part of that experimental study, focusing on the superelastic behavior of NiTi SMAs at various loading rates and temperatures, and heat treatment conditions. In addition, cyclic quasi-static and repeated dynamic loadings are used to examine the fatigue effect on the superelastic behavior of this material.

3. Dissipated energy in superelastic loop

When a sample of a NiTi SMA is subjected to a cycle of deformation within its superelastic strain range, it dissipates a certain amount of energy without a permanent strain, as is illustrated in Fig. 2 which shows a typical loading and unloading response of a sample in compression. In this figure, the area S_{ABCG} is the total energy input per unit initial volume during the loading, and the area of S_{FEDCG} is the energy release per unit volume during unloading. Thus, the dissipated energy, per unit initial volume, is given by

$$E_{\text{disp}} = S_{ABCG} - S_{FEDCG} = \oint_{S_{\text{loop}}} \sigma \, \mathrm{d}\varepsilon$$

where σ is the engineering stress, ε is the engineering (nominal) strain, and the integration is taken along the closed loop. The dissipated energy is due to phase transformation, from austenitic to martensitic, during loading and the reverse transformation back to austenitic in unloading, resulting in a net release of heat energy. This energy dissipation

property of SMAs may be used in shock and vibration mitigation.

In Fig. 2, σ_{tr} denotes the austenite to martensite transformation stress, defined by the intersection of the lines that are tangent to the initial elastic and the upper plateau of the loading stress–strain curve, and σ_{re} denotes the reverse martensite to austenite transformation stress.

4. Experiments

4.1. Material and specimens

The NiTi SMA material is obtained from Nitinol Devices & Components (NDC). The as-received wires are 4.75 mm in diameter, with initial condition of 42% cold work. Transformation temperature, A_f, of this NiTi material is about −10 °C when completely annealed according to the NDC suggestion. The chemical composition of the material is given in Table 1.

All samples are cut from the same NiTi alloy wire. The wire is machined into cylinders of 4.5 mm nominal diameter and 5 mm height. To reduce the end friction on the samples during the deformation, the sample ends are first polished using waterproof silicon carbide paper, 1200 and 4000 grit, then the samples are annealed at different desired temperatures, and finally, the ends are greased before the tests.

4.2. Annealing temperature effect on superelastic behavior

Different specimens made from the above-described NiTi SMA are annealed at different temperatures and durations in a furnace with an accuracy of ±2 °C. Then, the samples are compressed at a strain rate of 10^{-3}/s at room temperature, to a maximum strain of about 5.5%, using an Instron servohydraulic testing machine. The resulting stress–strain curves are shown in Fig. 3 for the indicated annealing temperatures; note that each test starts at zero strain, but the various curves are shifted horizontally for clarity in the display. Fig. 4 displays the forward and the reverse transformation stresses as functions of the annealing temperature. From this figure, it is seen that the transformation stresses, σ_{tr} and σ_{re}, of the NiTi SMA decrease with the increasing annealing temperature. The dissipated energy, E_{disp}, is plotted in Fig. 5 as a function of the annealing temperature. The dissipated energy, given by the area of the hysteresis loop, also changes with the annealing temperature. It attains a minimum at a 600 K annealing temperature, and a maximum at both 296 K (room temperature) and 873 K. With these two latter temperatures, a residual strain (RS) of about 0.85% is observed. If the annealing temperature is increased beyond 900 K, the NiTi SMA shows substantial irrecoverable strains. The stress–strain curve at an annealing temperature of 923 K actually is similar to that of an ordinary austenite

Table 1
The chemical composition of NiTi (wt.%)

Ni	O	H	C	Co	Cu	Fe	Ti
55.9	<0.0314	<0.002	0.0027	<0.005	<0.005	0.007	Balance

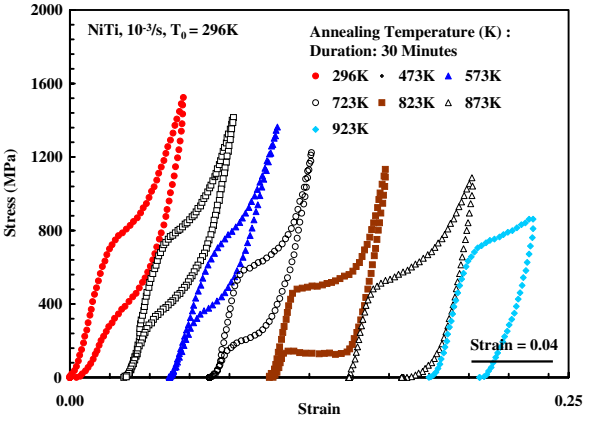

Fig. 3. Stress–strain curves at a strain rate of 10^{-3}/s and 296 K temperature, for indicated annealing temperatures and 30 min duration; each test starts at zero strain.

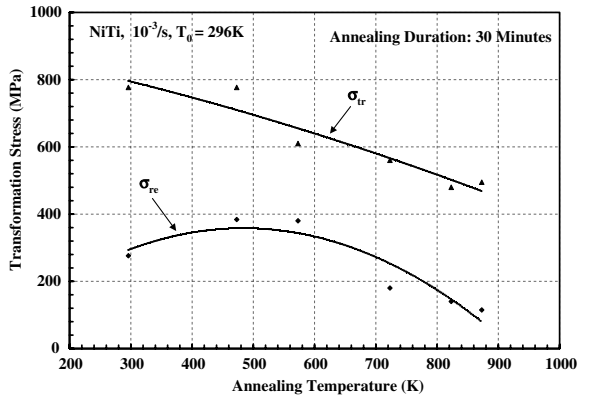

Fig. 4. Transformation stress as a function of annealing temperature.

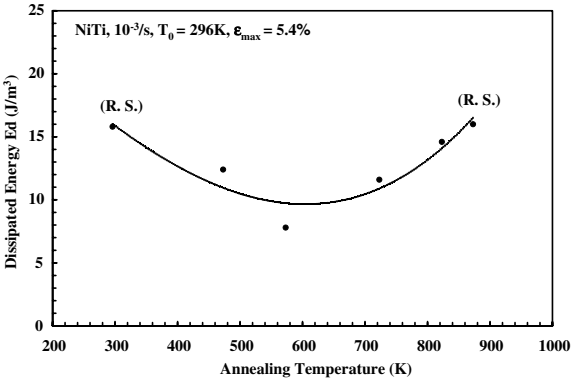

Fig. 5. Dissipated energy as a function of annealing temperature.

steel. To obtain the results shown in Fig. 6, the annealing duration has been changed, keeping the annealing temperature at 473 K. It is seen that the annealing duration does not seem to affect the superelastic behavior of the material at this low temperature.

Based on the experimental observations, we may make the following observations:

(1) The annealing temperature has a significant effect on the superelastic behavior of NiTi SMAs. The transformation stresses, σ_{tr} and σ_{re}, and the dissipated energy, E_{disp}, change with the annealing temperature.
(2) The dissipated energy, E_{disp}, attains a minimum when the annealing temperature reaches about 600 K; it can thus be maximized by adjusting the annealing temperature.
(3) Although the transformation stress, σ_{tr}, of NiTi SMAs increases with the decreasing annealing temperature, it also induces a greater residual strain.
(4) When the annealing temperature is about 923 K, the material actually is no longer superelastic.
(5) The annealing duration (at a temperature of 473 K) has a weak effect on the superelastic behavior as compared with that of the annealing temperature.

4.3. Irrecoverable strain in NiTi SMAs

Examining the results in Figs. 3–5, it is seen that the transformation stress, σ_{tr}, and the dissipated energy, E_{disp}, both attain maximum values for the annealing temperature of about 473 K. The values of σ_{tr} and E_{disp} are closely related to the superelastic strain of the material.

To measure the irrecoverable strain, samples are annealed at 473 K for 30 min, and are compressed at a strain rate of 10^{-3}/s and 296 K. The results are shown in Fig. 7. For a maximum strain of about 6%, the residual strain is about 0.5%. Fig. 8 shows the results of compression tests on three other samples, with the maximum strain of about 6%, attained at a strain rate of 10^{-3}/s. It is seen that when the test temperature is 296 K, the residual strain is 0.5%, whereas when the test temperature is 273 K, the residual strain is 0.25%, and when the test temperature is further reduced to 253 K, the residual strain becomes 0.5% again. Therefore, when the annealing temperature is 473 K, a good superelastic property (smaller residual strain) is found at a test temperature of 273 K for a strain rate of 10^{-3}/s. The results in Fig. 9 show that, if samples are compressed to a

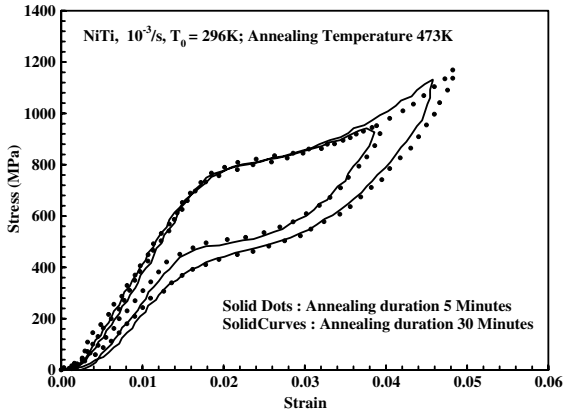

Fig. 6. Effect of annealing duration on superelastic behavior.

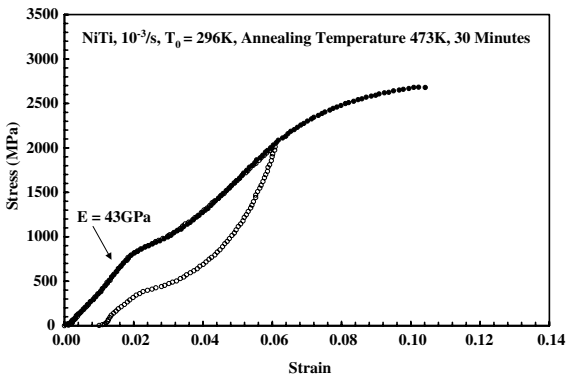

Fig. 7. Stress–strain curve at indicated annealing temperature and duration.

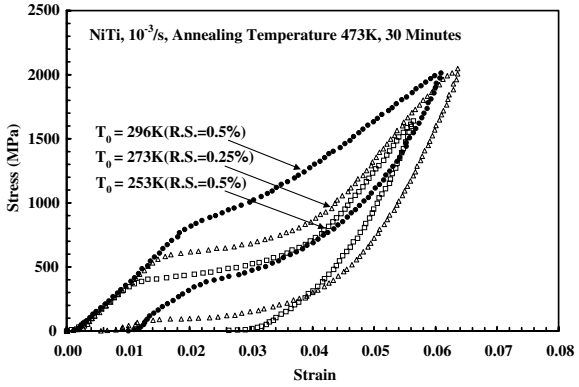

Fig. 8. Stress–strain curves at a strain rate of 10^{-3}/s and indicated test temperatures.

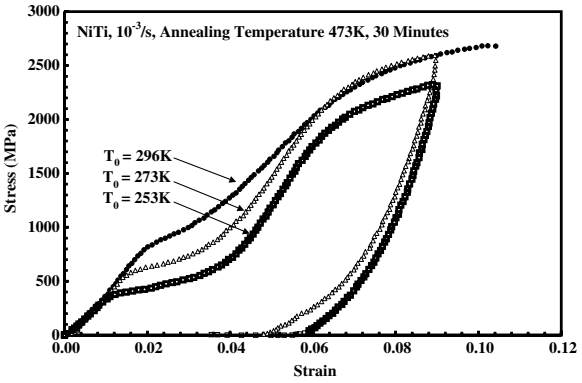

Fig. 9. Residual strains at indicated test temperatures.

strain of about 8.4% at a strain rate of 10^{-3}/s, then the irrecoverable strain for test temperatures of 253 and 273 K is about 3%. As is discussed later on, for 30 min annealing at 823 K, three cycles of straining to 5.8% maximum strain result in zero residual strain (see Fig. 10), but a fourth cycle to 8% maximum strain results in a 4% residual strain. A similar irrecoverable strain is observed for 30 min annealing at 473 K. Based on these results, we infer that this NiTi SMA could have a recoverable strain up to about 6% maximum strain.

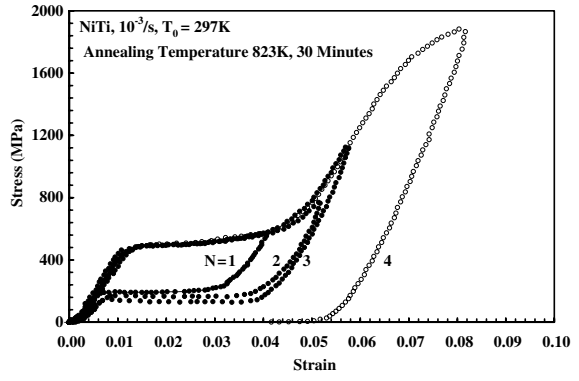

Fig. 10. Change in superelasticity due to repeated loading.

4.4. Dissipated energy, E_{disp} in cyclic loading

SMAs possess high damping capacity both in the austenite state as a result of the stress-induced martensitic transformation, and in the martensite state as a result of the stress-induced martensitic variant reorientation (Liu et al., 1999a,b). Following Fig. 2, in near-equiatomic Ti–Ni alloys the thermoelastic martensitic transformation from the parent phase with a B2 structure to a monoclinic B19′ structure occurs upon loading, then the thermoelastic martensitic transformation from the B19′ to the B2 structure occurs upon unloading. By deformation cycling in the superelastic temperature range (above A_f), the shape of the recovery superelastic loop in the stress–strain curve changes gradually; the yield stress and the hysteresis width of the loop decrease, and the permanent elongation increases. Although the change in the shape of the superelastic loop is significant in the early cycles, it becomes insignificant after 100 cycles (Saburi, 1998). The cycle of superelastic deformation affects the critical stress to start the stress-induced transformation (Kato et al., 1999). Cycling at higher strain rates has been found to increase the residual elongation that remains after the specimen is unloaded, and to cause a more rapid decline of the critical stress for martensite formation (Strnadel et al., 1995).

Several NiTi SMA samples are first annealed at 773 K for 30 min, then they are compressed repeatedly to a common maximum stress at various temperatures. The curves in Fig. 11 are at a 296 K test temperature. Their corresponding energy and residual strain vs. the number of cycles are shown in Fig. 12. In this figure, the dissipated energy, E_{disp} decreases and tends to a stable value with an increasing number of cycles. The accumulated residual strain also increases gradually and attains a stable value, as the number of cycles increases. The change in the superelastic loop is significant in several of the early cycles, as also reported by Saburi (1998). The stress–strain curves in Fig. 13 are at a 326 K test temperature. These show that initially the shape of the superelastic loops is almost the same, but it begins to change after the

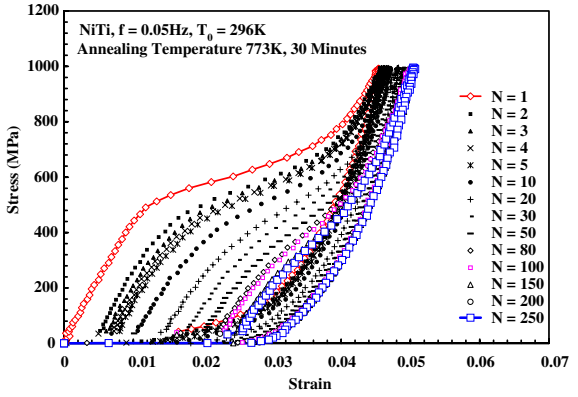

Fig. 11. Stress–strain curves in cyclic loading of 0.05 Hz at 296 K.

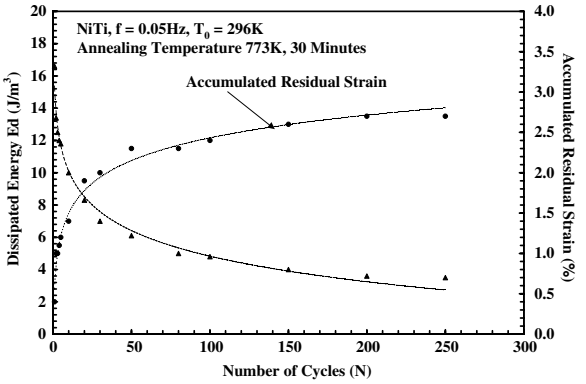

Fig. 12. Dissipated energy, and accumulated residual strain vs number of cycles.

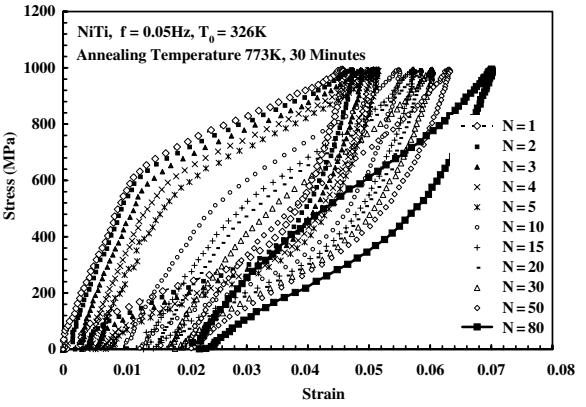

Fig. 13. Stress–strain curves in cyclic loading of 0.05 Hz frequency.

fifth cycle. The corresponding energy and the residual strain are shown in Fig. 14 as functions of the

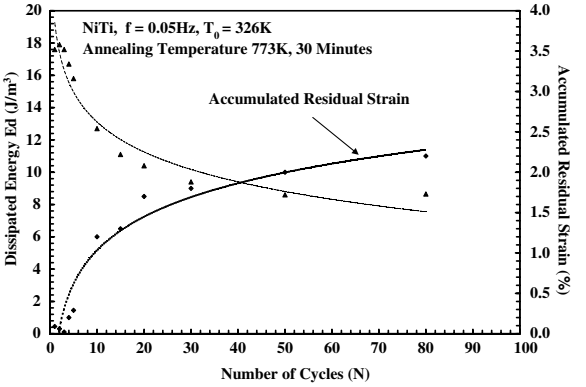

Fig. 14. Dissipated energy, and accumulated residual strain vs number of cycles.

number of cycles. Comparing curves in Fig. 14 with those in Fig. 12, it is seen that the shape of the superelastic loop, the dissipated energy, E_{disp}, and the accumulated residual strain tend to their stable values much sooner at 326 K than at 296 K. In Figs. 11 and 13, the stress–strain curves shift to the right due to the accumulated residual strain. According to Figs. 11–14, the dissipated energy, first quickly decreases, and then E_{disp}, gradually tends to its stable value, while the accumulated residual strain first increases rapidly and then gradually tends to its stable value, as the number of fatigue cycles increases. In practice, SMAs are repeatedly deformed to obtain stable and well behaved superelastic behavior. This is usually called the "training process." In general, repeated training results in smaller dissipated energy for SMAs. In the present tests, the dissipated energy is greater at a 326 K test temperature than at 296 K. In Fig. 15, the sample is annealed at a temperature of 473 K for 30 min, then tested. As can be seen, the residual strain in the first cycle is quite large, but in the 100th cycle, the increment of residual strain for that cycle basically disappears. The dissipated energy also decreases rather rapidly as the number of cycles increase.

Based on the above results, it is seen that (1) the energy dissipated in each cycle of loading–unloading of NiTi SMAs decreases, and even disappears as the number of cycles increases; similarly, the accumulated residual strain tends to a stable value with an increasing number of fatigue cycles; and (2) the residual strain depends on the test temperature, the fatigue stress amplitude, and the annealing temperature.

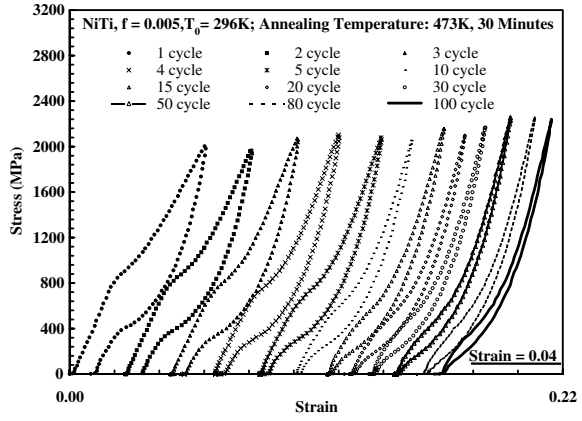

Fig. 15. Stress–strain curves for the last cycle of indicated loading frequency; each curve starts at zero strain.

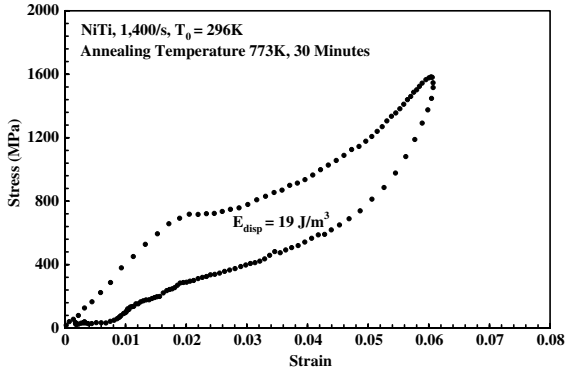

Fig. 16. A typical dynamic stress–strain curve for NiTi SMA at 1400/s loading strain rate and 296 K initial temperature.

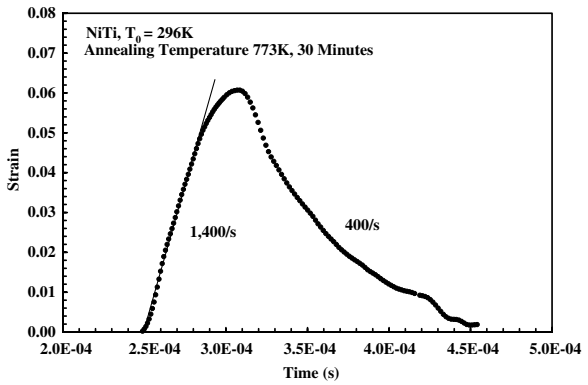

Fig. 17. A typical dynamic strain time history obtained using the Hopkinson bar technique.

5. Strain rate effect

In general, the elastic properties of metals are temperature dependent, and high strain rate loading can lead to a temperature rise in the material. For the superelastic deformation of NiTi SMAs, a small temperature change can produce a change in the superelastic behavior, as in Figs. 8 and 9. In the present study, dynamic tests at high-strain rates (greater than 10^2/s), and initial temperatures in the range of 77–400 K, are performed using UCSD's recovery Hopkinson bar facility, enhanced for high-temperature and high-strain rate recovery tests (Nemat-Nasser et al., 1991; Nemat-Nasser and Isaacs, 1997). With this facility, the reflected tensile pulse in the incident bar is trapped, so that the sample is subjected to a single compression pulse of desired profile, as discussed by Nemat-Nasser et al. (1991).

5.1. Superelastic response

Several specimens are annealed at 773 K for 30 min, and then tested at various strain rates, using UCSD's recovery Hopkinson technique with a paper pulse shaper. The result of one such test is displayed in Fig. 16. The transformation stresses, σ_{tr} and σ_{re}, for this case are 720 MPa and 280 MPa, respectively, and the dissipated energy is 19 J/m^3, with an average strain rate of 1400/s, at a 296 K initial temperature. The sample deformation is completely recovered in this test. The unloading occurs at a lower strain rate than that of loading. The strain time history is plotted in Fig. 17. By calculating the slope of the loading and unloading curves, the unloading strain rate is about 400/s, whereas the loading occurs at a 1400/s strain rate. We have observed in all our tests that the unloading for NiTi SMAs occurs at a strain rate of the order of 10^2/s, independently of the loading rates. In general, the unloading rate cannot be easily controlled. Therefore, hereafter we focus attention on the loading rates only.

5.2. Superelastic behavior in dynamic fatigue tests

Our quasi-static cyclic loadings show that the dissipated energy, E_{disp}, of NiTi SMAs tends to a stable value with an increasing number of cycles. This value depends on the maximum strain and the stress level. To explore the high strain rate superelastic behavior of NiTi SMAs under repeated loading, dynamic tests are performed using UCSD's recovery Hopkinson bar facility. The experimental pro-

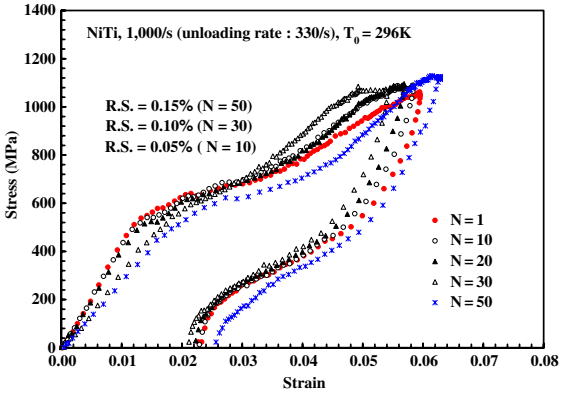

Fig. 18. Stress–strain curves at 1000/s loading strain rate and 296 K initial temperature.

cess is similar to that in subsection 6.1. A sample is repeatedly loaded for 50 cycles, each to a maximum strain of about 5.6%, at a 1000/s strain rate and a 296 K initial testing temperature; see Fig. 18. In the figure, the unloading curves do not completely return to the origin. However, precise dimensional measurement reveals an almost complete recovery after each unloading, indicating that full recovery has been attained shortly after the stress–strain measurement was terminated. For a typical case, after 10 cycles, the accumulated residual strain is about 0.05%, and after 50 cycles, it is about 0.15%. The dissipated energy for each cycle is about 22 J/m^3. Compared with the results of the quasi-static case, the dissipated energy, E_{disp}, remains almost a constant in the dynamic case.

5.3. Strain rate effect on superelastic behavior

In general, the NiTi SMAs in the austenite phase are cubic with high crystal symmetry. Upon stressing, the cubic austenite phase transforms into a lower symmetry monoclinic phase (martensite). Upon unloading, the martensitic phase transforms back into the austenitic phase, since the martensitic phase is not stable. This is a diffusionless phase transformation in solids, in which atoms move cooperatively, and often by a shear-like mechanism. This kind of transformation is sometimes referred to as displacive or military transformation. One open problem is the relation between this transformation and the applied strain rate. In this paper, in order to understand the strain rate effect on the superelastic behavior of the NiTi SMAs, we compare our low strain rate results with those of high strain rates (greater than 10^2/s), obtained using UCSD's enhanced Hopkinson technique. Six samples are uniaxially compressed at various loading strain rates and a 296 K initial temperature, and the results are shown in Fig. 19. It is seen that the transformation stresses, σ_{tr}, and σ_{re} increase with the increasing strain rate. The plateau range (austenite to martensite transformation region) tends to disappear as the strain rate reaches 4200/s. For strain rates in the range of 0.1–2100/s, the loading portion of the stress–strain curves appears to be similar, as in Fig. 20, but the stress levels are quite different, being greater for the higher strain rate; for a systematic study of the effect of strain rate on the response of SMAs, see Nemat-Nasser et al. (2005a,b). As shown by these authors, for very high strain rates, the response of this material is similar to that of an ordinary metal. The result for a strain rate of

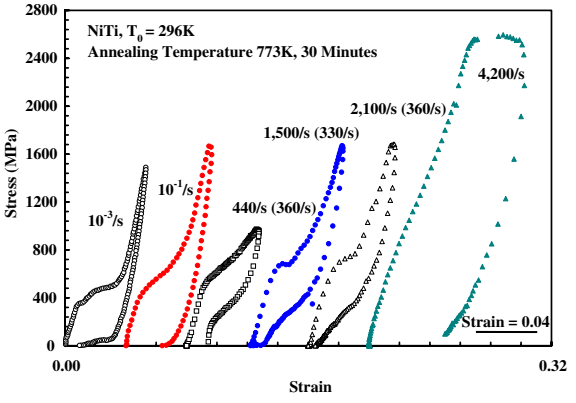

Fig. 19. Stress–strain curves at indicated loading strain rates and 296 K initial temperature; each curve starts at zero strain.

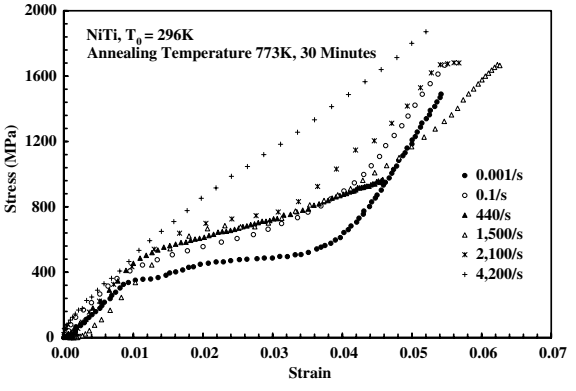

Fig. 20. Stress-induced martensitic transformation (austenite to martensite) curves at indicated loading strain rates and 296 K initial temperature.

4200/s in Fig. 20, seems to suggest this tendency. Thus, with increasing stress level or strain rate, the diffusionless shear-like mechanism of deformation changes to dislocation-based slip plasticity (Nemat-Nasser and his coworkers, 2005a,b). Therefore, when the strain rate increases to 4200/s and higher, the NiTi SMA tends to deform essentially similar to an ordinary austenite metal.

5.4. Temperature effect on superelastic behavior

In general, the parent phase (austenite) of SMAs is stable at temperatures greater than A_f. Thus, greater applied stresses are required for stress-induced martensitic transformation at such temperatures. Figs. 21 and 22 show the effect of temperature on the plateau stress for samples loaded at 10^{-3}/s strain rate. The plateau disappears for a 396 K initial test temperature. A similar response is observed at high strain rates (Fig. 20, 4200/s strain rate). This shows that above a critical temperature (here higher than 396 K) the parent phase is so stable that stressing cannot induce martensitic transformation. The transformation stresses, σ_{tr} and σ_{re}, of the NiTi SMAs tend to increase with increasing temperature, as does the residual strain; see results in Figs. 21 and 22. In Figs. 23 and 24, the stress–strain curves are plotted at different temperatures for 0.1/s and 1400/s strain rates. The trend of these curves is the same as those of Figs. 21 and 22. The plateau slope of the stress–strain curves increases with increasing temperature. For a temperature of 356 K and a 1400/s strain rate, the stress-induced martensitic transformation is essentially suppressed (see Fig. 24). In Fig. 25, the loading parts of the curves in Fig. 24 are plotted

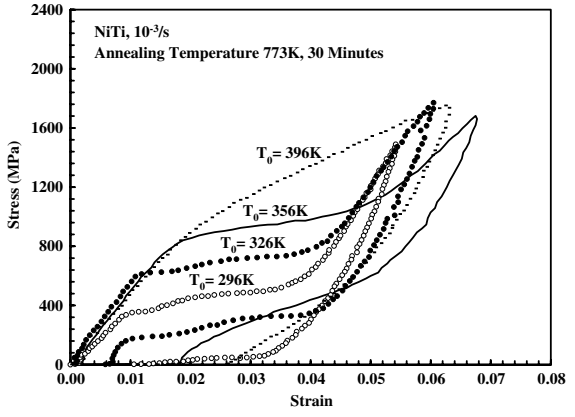

Fig. 21. Stress–strain curves at 10^{-3}/s strain rate and 296, 326, 356, and 396 K initial temperatures.

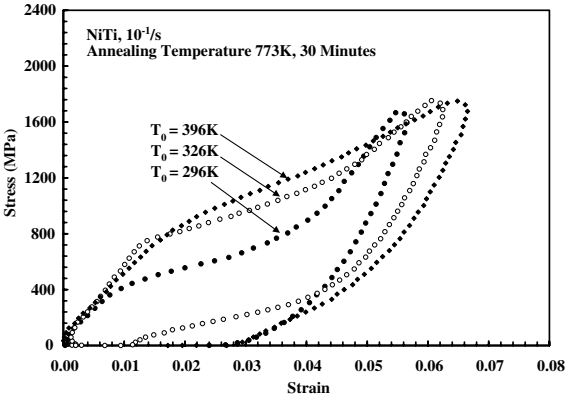

Fig. 23. Stress–strain curves at 10^{-1}/s strain rate and 296, 326, and 396 K temperatures.

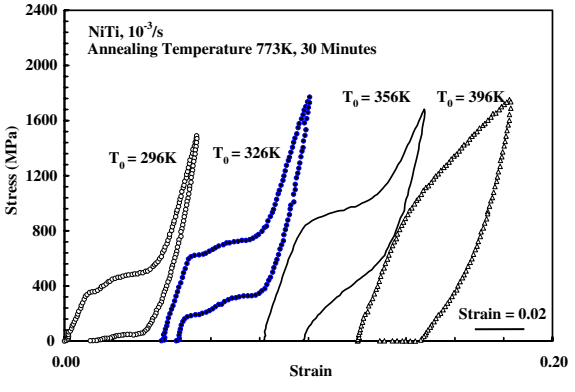

Fig. 22. Stress–strain curves at 10^{-3}/s strain rate and indicated initial temperatures; each curve starts at zero strain.

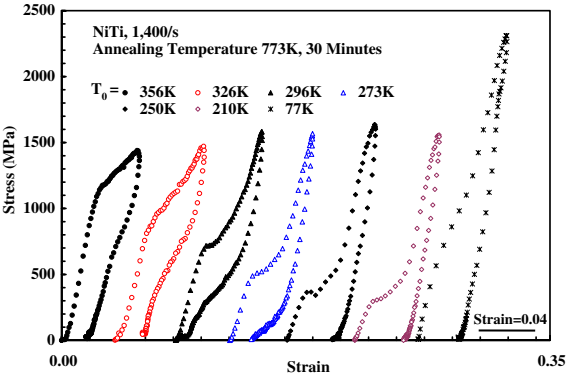

Fig. 24. Stress–strain curves at 1400/s loading strain rate and indicated initial temperatures; each test starts at zero strain.

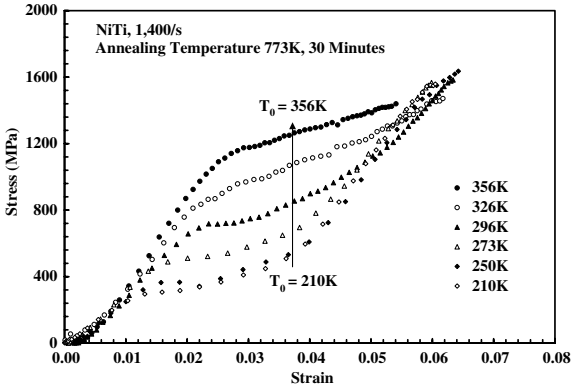

Fig. 25. Stress-induced martensitic transformation (austenite to martensite) at 1400/s loading strain rate and indicated initial temperatures.

and compared. As is evident, the transformation stress, σ_{tr}, increases with increasing temperature.

6. Conclusions

To understand the thermomechanical response, especially the superelastic behavior of NiTi shape-memory alloys (SMAs), a number of uniaxial compression tests are performed using an Instron servohydraulic testing machine and UCSD's enhanced Hopkinson technique. These tests are performed over the range of strain rates from 10^{-3}/s to about 4200/s, and at various initial temperatures, up to 400 K. The influence of the annealing temperature on the fatigue response is also examined. Several noteworthy conclusions are as follows:

(1) By changing the annealing temperature, the transformation stress and the dissipated energy of NiTi SMAs can be obviously changed, as this changes the transformation temperatures.
(2) In the quasi-static cyclic fatigue tests, the dissipated energy of NiTi SMAs tends to a minimum stable value, and the cyclic loading can lead to a stable superelastic behavior for the SMAs.
(3) Dynamic repeated tests of NiTi SMAs result in a smaller change in the shape of the superelastic loop and the dissipated energy than the quasi-static cyclic tests.
(4) The split Hopkinson bar can be effectively used for high loading rates, but, the unloading rate in this system cannot be easily controlled; it has been of the order of 10^2/s in our tests.

Acknowledgments

This work was supported by ONR grant N00014-02-1-0666 to the University of California, San Diego.

References

Chen, W.W., Wu, Q., Kang, J.H., Winfree, N.A., 2001. Compressive superelastic behavior of a NiTi shape memory alloy at strain rates of 0.001–750 s^{-1}. Int. J. Solids Struct. 38, 8989–8998.

Gadaj, S.P., Nowacki, W.K., Pieczyska, E.A., 2002. Temperature evolution in deformed shape memory alloy. Infrared Phys. Technol. 43, 151–155.

Gall, K., Sehitoglu, H., Chumlyakov, Y.I., Kireeva, I.V., 1999. Tension-compression asymmetry of the stress–strain response in aged single crystal and polycrystalline NiTi. Acta Mater. 47 (4), 1203–1217.

Hosogi, M., Okabe, N., Sakuma, T., Okita, K., 2002. A new constitutive equation for superelastic deformation and prediction of martensite volume fraction in Titanium–Nickel–Copper shape memory alloy. Mater. Trans. JIM 43 (5), 822–827.

Huang, X., Liu, Y., 2001. Effect of annealing on the transformation behavior and superelasticity of NiTi shape memory alloy. Scripta Mater. 45, 153–160.

Kato, H., Ozu, T., Hashimoto, S., Miura, S., 1999. Cyclic stress–strain response of superelastic Cu–Al–Mn alloy single crystal. Mater. Sci. Eng. A A264, 245–253.

Lagoudas, D.C., Ravi-Chandar, K., Sarh, K., Popov, P., 2003. Dynamic loading of polycrystalline shape memory alloy rods. Mech. Mater. 35, 689–716.

Liu, Y., Li, Y., Ramesh, K.T., Humbeeck, J.V., 1999a. High strain rate deformation of martensitic NiTi shape memory alloy. Scripta Mater. 41 (1), 89–95.

Liu, Y., Xie, Z., Humbeeck, J.V., 1999b. Cyclic deformation of NiTi shape memory alloys. Mater. Sci Eng. A A273–A275, 673–678.

Miller, D.A., Lagoudas, D.C., 2001. Influence of cold work and heat treatment on the shape memory effect and plastic strain development of NiTi. Mater. Sci. Eng. A A308, 161–175.

Nemat-Nasser, S., Isaacs, J.B., 1997. Direct measurement of isothermal flow stress of metals at elevated temperatures and high strain rates with application to Ta and Ta–W alloys. Acta Mater. 45, 907–919.

Nemat-Nasser, S., Isaacs, J.B., Starrett, J.E., 1991. Hopkinson techniques for dynamic recovery experiments. Proc. R. Soc. Lond. 435 (A), 371–391.

Nemat-Nasser, S., Choi, J.Y., Guo, W.-G., Isaacs, J.B., 2005a. Very high strain-rate response of a NiTi shape-memory alloy. Mech. Mater. 37, 287–298.

Nemat-Nasser, S., Choi, J.Y., 2005b. Strain rate dependence of deformation mechanisms in a Ni–Ti–Cr shape-memory alloy. Act Mater. 53, 449–454.

Otsuka, K., Ren, X., 1999. Recent development in the research of shape memory alloys. Intermetallics 7, 511–528.

Otsuka, K., Wayman, C.M., 1998. Mechanism of shape memory effect and superelasticity. In: Otsuka, K., Wayman, C.M.

(Eds.), Shape Memory Materials. Cambridge University Press, Cambridge, pp. 27–48.

Saburi, T., 1998. TiNi shape memory alloys. In: Otsuka, K., Wayman, C.M. (Eds.), Shape Memory Materials. Cambridge University press, Cambridge, pp. 49–96.

Shaw, J.A., Kyriakides, S., 1995. Thermomechanical aspects of NiTi. J. Mech. Phys. Solids 43 (8), 1243–1281.

Strnadel, B., Ohashi, S., Ohtsuka, H., Miyazaki, S., Ishihara, T., 1995. Effect of mechanical cycling on the pseudoelasticity characteristics of Ti–Ni and Ti–Ni–Cu alloys. Mater. Sci. Eng. A A203, 187–196.

Tobushi, H., Shimeno, Y., Hachisuka, T., Tanaka, K., 1998. Influence of strain rate on superelastic properties of NiTi shape memory alloy. Mech. Mater. 30, 141–150.